EXTENSION OF THE J INTEGRAL TO 3D FRACTURE MECHANICS AND APPLICATIONS IN ENGINEERING

A. Frediani, D. Vecchiatini*

The Crack Driving Force along the front of a 3D crack can be written in the form of a Generalized J Integral,given by the contributions of a line integral and a surface integral. In order to evaluate these integrals by the Finite Element method,a suitable algorithm has been set up and implemented in a computer program.In the present paper the preliminary examples discussed are a penny-shaped crack,elliptical embedded and surface cracks and a Compact Tension specimen. The results obtained in this paper show that the evaluation of the Generalized J Integral by the F.E.method is simple,reliable and that no mesh refinement is necessary.

INTRODUCTION

The application of Fracture Mechanics to the design of structures has been remarkably successful in the case of plane strain and plane stress problems,where a crack is characterized by a single parameter,that is,crack length;in these situations,Linear Elastic Fracture Mechanics is currently used and the numerical methods available provide solutions in terms of the Stress Intensity Factor, which are considered to be fairly accurate in all the significant design conditions.

In tridimensional problems,a crack is characterized by a "shape"; in general,S.I.F. varies along the crack front and the use of numerical methods to calculate this local value of S.I.F. is expensive and, sometimes,results are questionable.Considerable attention has been devoted to the computational problems in 3D Linear Elastic Fracture Mechanics and different methodologies (Direct methods of Forces and displacements,Virtual Crack Extension,Stiffness Derivatives) or different elements (Crack Tip or Isoparametric elements) are available;problems arise in engineering applications,where the great mesh refinement around the crack front,which is necessary in order to obtain reliable results,gives rise to so large a number of

* Dipartimento di Ingegneria Aerospaziale, Università di Pisa.

degrees of freedom that the F.E.models become complex and expensive. Measurement of the Crack Driving Force without concentrating attention on the crack tip region was first proposed by Rice (1), who defined the well known J Integral in the presence of plane stress or strain states and without body forces. Later, certain extensions of the Rice's J Integral were proposed in order to include, for example, the effects of temperature, body forces (Sakata et al (2)) and concentrated loads in a plate (Frediani et al (3)), but a very important improvement in Fracture Mechanics consisted in the measurement of the Crack Driving Force in 3D problems by means of integral quantities, according to Rice's position.

Indeed, the measurement of the Crack Driving Force at any point of a tridimensional crack can be written as the sum of a line integral and a surface integral. The line integral (or, simply, J_L) is defined along any path which belongs to a plane normal to the crack front at the point in question; the expression of the relevant integration function is the same as Rice's J Integral. The surface integral (J_A) is defined on the surface included in the previous path and disappears in plane stress and plane strain; in this way, a Generalized J Integral (or GJ, for the sake of brevity in the rest of the paper) is defined.

Up till now, the only disadvantages in the utilization of GJ as the main parameter in Fracture Mechanics are the serious problems arising when this integral has to be evaluated (Bakker (4)). This paper shows how to carry out this evaluation and indicates certain consequences of this result for the future.

THE GENERALIZED J INTEGRAL

Let us consider a homogeneous body with a plane crack, limited by a continuous curve γ along which the first derivative is defined virtually everywhere; for the sake of simplicity, we suppose that surface forces alone are present, even though other loading conditions have been considered in the literature by Wang (5) for example.

Let P(s) be a point on γ, where "s" is a curvilinear coordinate and $\underset{\sim}{\tau}(s)$ and $\underset{\sim}{\mu}(s)$ are, respectively, normal and tangent unit vectors to γ in P(s) (Fig.1); the Crack Driving Force in P, relevant to crack growth in the $\underset{\sim}{\mu}$ direction, can be written as

$$G(P(s))=\underset{\sim}{\mu}\cdot\int_{\Gamma}[w\underset{\sim}{1}-(\nabla\underset{\sim}{u})^T\underset{\sim}{S}]\underset{\sim}{n}\,dS-\int_{A}\frac{\partial}{\partial\underset{\sim}{\tau}}[\underset{\sim}{S}\underset{\sim}{\tau}\cdot(\nabla\underset{\sim}{u})\underset{\sim}{\mu}\,dA \quad (=GJ)\ .\ .\ . \qquad (1)$$

where: w is the strain energy density, (∇u) is the gradient of the displacement vector $\underset{\sim}{u}$, $\underset{\sim}{S}$ is the stress tensor (Piola Kirchhoff tensor), Γ is an integration path and A is the surface included in Γ according to fig.1.

The right-hand side term in (1) is the GJ integral; in the case of plane stress and plane strain states, γ is a straigth line and we

---

An interesting proof of eqn.(1) is to be found in Bennati (6) get:

$$\frac{\partial}{\partial \underset{\sim}{\tau}}\left[\underset{\sim}{S}\underset{\sim}{\tau}\cdot\nabla\underset{\sim}{u}\;\underset{\sim}{\mu}\right]=0 \qquad (2)$$

and, consequently, the expression of the Crack Driving Force becomes

$$G(P)=\underset{\sim}{\mu}\int_{\Gamma}\left[w\underset{\sim}{1}-(\nabla\underset{\sim}{u})^{T}\underset{\sim}{S}\right]\underset{\sim}{n}dS \quad (=J) \qquad (3)$$

where J is the Rice's J Integral.

COMPUTATION OF THE GJ INTEGRAL BY THE F.E. METHOD

According to eqn. (1), the GJ integral can be defined on the basis of two terms : a line integral along a path $\Gamma(J_L)$ and a surface integral in the domain A (J_A), so that

$$GJ = J_L - J_A. \qquad (4)$$

J_L depends on stresses and displacements, while J_A depends on the derivatives of these quantities.

Even though large deformations and constitutive equations of non-linear materials can be used in the assessment of GJ, the hypotheses of linear elastic materials and small deformations are used in the present F.E. computations in order to simplify the problem and to possibly compare the results obtained with those existing in the literature.

Displacements and stresses are obtained as a direct result of F.E. analysis and, therefore, the quantity J_L can be immediately computed; the opposite occurs as far as J_A is concerned and the problem arises of evaluating second derivatives of displacements (the terms of J_A) on the basis of the displacements and the first derivatives of them (the results of F.E. analysis).

This problem is solved in the isoparametric space and by formulating a suitable algorithm in order to assess all the terms of J_A in the isoparametric coordinates.

The twenty node isoparametric elements are commonly utilized in Fracture Mechanics; typical advantages of this are those connected with the simple interpolation functions used, with the possibility of simulating stress singularities by the Quarter Point Node Technique, and with the presence of these elements in general purpose codes, etc, but, in the present context, the main advantage is the possibility of expressing the integration functions of J_L and J_A in the isoparametric coordinates.

The correspondence between the coordinates (x,y,z) of a material point in a body and the isoparametric coordinates (ξ,η,ζ) of a twenty node isoparametric element is expressed by:

$$x = \sum_{1}^{20} N_i(\xi,\eta,\zeta)x_i$$

$$y = \sum_{1}^{20} N_i(\xi,\eta,\zeta)y_i \qquad (5)$$

$$z = \sum_{1}^{20} N_i(\xi,\eta,\zeta)z_i$$

where N_i is a shape function and (x_i,y_i,z_i) are the coordinates of the i.th node; similar relationships are valid as far as displacements are concerned:

$$u = \sum_{1}^{20} N_i(\xi,\eta,\zeta)u_i$$

$$v = \sum_{1}^{20} N_i(\xi,\eta,\zeta)v_i \qquad (6)$$

$$w = \sum_{1}^{20} N_i(\xi,\eta,\zeta)w_i$$

where (u_i,v_i,w_i) are displacement components of the i^{th} node.
The Jacobian matrix of (5) and the inverse of it are, respectively:

$$J = \begin{bmatrix} \frac{\partial x}{\partial \xi} & \frac{\partial y}{\partial \xi} & \frac{\partial z}{\partial \xi} \\ \frac{\partial x}{\partial \eta} & \frac{\partial y}{\partial \eta} & \frac{\partial z}{\partial \eta} \\ \frac{\partial x}{\partial \zeta} & \frac{\partial y}{\partial \zeta} & \frac{\partial z}{\partial \zeta} \end{bmatrix} \qquad J^{-1} = \begin{bmatrix} \frac{\partial \xi}{\partial x} & \frac{\partial \eta}{\partial x} & \frac{\partial \zeta}{\partial x} \\ \frac{\partial \xi}{\partial y} & \frac{\partial \eta}{\partial y} & \frac{\partial \zeta}{\partial y} \\ \frac{\partial \xi}{\partial z} & \frac{\partial \eta}{\partial z} & \frac{\partial \zeta}{\partial z} \end{bmatrix} \; ; \qquad (7)$$

The terms of the matrix J are known functions of the isoparametric coordinates; the expressions of the terms of the J^{-1} matrix in terms of (ξ,η,ζ) are obtained as shown in App.I and are fundamental in order to evaluate the J_A surface integral.
The finite element mapping in the crack front region is carried out according to the following procedure:

1) fix a global reference system (x_G,y_G,z_G) so that, for example, the crack belongs to the (x_G,y_G) plane (fig.2);
2) estabilish a set of control points, P, on the crack front γ;
3) at any point P consider the aforementioned "local" reference system (x,y,z), where:
   - the origin is conventionally fixed in the x_G axis,
   - the plane (x,y) is normal to the unit vector τ, tangent to γ in P,
4) design the finite element mesh so that the (x,y) plane contains the Gauss Points of the elements included in the path Γ.

Concerning this local reference system, the expressions of J_L and J_A are the following:

$$J_L = \int_{\Gamma} \{ \frac{1}{2}(\sigma_x\varepsilon_x + \sigma_y\varepsilon_y + \sigma_z\varepsilon_z + \tau_{xy}\gamma_{xy} + \tau_{zy}\gamma_{zy} + \tau_{zx}\gamma_{zx})dy - [(\sigma_x n_x + \tau_{xy}n_y + \tau_{xz}n_z) \frac{\partial u}{\partial x} + (\tau_{xy}n_x + \sigma_y n_y + \tau_{yz}n_z)\frac{\partial v}{\partial x} + (\tau_{zx}n_x + \tau_{zy}n_y + \sigma_z n_z)\frac{\partial w}{\partial x}] ds \} \qquad (8)$$

$$J_A = \int_A \left(\frac{\partial \tau_{xz}}{\partial z} \frac{\partial u}{\partial x} + \tau_{xz} \frac{\partial^2 u}{\partial x \partial z} + \frac{\partial \tau_{yz}}{\partial z} \frac{\partial v}{\partial x} + \tau_{yz} \frac{\partial^2 v}{\partial x \partial z} + \frac{\partial \sigma_z}{\partial z} \frac{\partial w}{\partial x} + \right.$$

$$\left. + \sigma_z \frac{\partial^2 w}{\partial x \partial z} \right) dA \; ; \qquad (9)$$

n_x, n_y, n_z are components of the unit vector $\underset{\sim}{n}$, normal to Γ (where $n_z = 0$ identically) and the other symbols have the usual meaning.

Evaluation of J_L. With the exception of $\partial v/\partial x$ and $\partial w/\partial x$, all the terms in (8) are directly obtained as outputs of F.E. computation in the isoparametric space and the cross derivatives $\partial v/\partial x$ and $\partial w/\partial x$ are obtained by differentiating the shape functions; therefore, the integration function of J_L is defined in terms of isoparametric coordinates and line integration along the path Γ can be carried out by means of the Gauss technique in the isoparametric space.
The integration paths are defined along the Gauss Points of the element involved.

Evaluation of J_A. In order to write the integration function of J_A in terms of isoparametric coordinates (ξ, η, ζ), certain mathematical operations must be carried out; as an example, let us consider the first term in (9): $(\partial \sigma_{xz}/\partial z)(\partial u/\partial x)$.
The derivative $\partial u/\partial x$ is an output of F.E.; for linear elastic materials, we have:

$$\frac{\partial \sigma_{xz}}{\partial z} = G\left(\frac{\partial^2 u}{\partial z^2} + \frac{\partial^2 w}{\partial x \partial z} \right)$$

and, obviously:

$$\frac{\partial^2 u}{\partial z^2} = \frac{\partial}{\partial z} \left(\frac{\partial (\Sigma N_i u_i)}{\partial \xi} \right) \frac{\partial \xi}{\partial z} + \frac{\partial (\Sigma N_i u_i)}{\partial \xi} \frac{\partial^2 \xi}{\partial z^2} +$$

$$+ \frac{\partial}{\partial z} \left(\frac{\partial (\Sigma N_i u_i)}{\partial \eta} \right) \frac{\partial \eta}{\partial z} + \frac{\partial (\Sigma N_i u_i)}{\partial \eta} \frac{\partial^2 \eta}{\partial z^2} +$$

$$+ \frac{\partial}{\partial z} \left(\frac{\partial (\Sigma N_i u_i)}{\partial \zeta} \right) \frac{\partial \zeta}{\partial z} + \frac{\partial (\Sigma N_i u_i)}{\partial \zeta} \frac{\partial^2 \zeta}{\partial z^2}$$

$$\frac{\partial^2 w}{\partial x \partial z} = \frac{\partial}{\partial x} \left(\frac{\partial \Sigma N_i w_i}{\partial \xi} \right) \frac{\partial \xi}{\partial z} + \frac{\partial \Sigma N_i w_i}{\partial \xi} \frac{\partial^2 \xi}{\partial x \partial z} +$$

$$+ \frac{\partial}{\partial x} \left(\frac{\partial \Sigma N_i w_i}{\partial \eta} \right) \frac{\partial \eta}{\partial z} + \frac{\partial \Sigma N_i w_i}{\partial \eta} \frac{\partial^2 \eta}{\partial x \partial z} +$$

$$+ \frac{\partial}{\partial x}\left(\frac{\partial \Sigma N_i w_i}{\partial \zeta}\right) \frac{\partial \zeta}{\partial z} + \frac{\partial (\Sigma N_i w_i)}{\partial \zeta} \frac{\partial^2 \zeta}{\partial x \partial z} \quad ;$$

finally,the derivatives $\partial\xi/\partial x$, $\partial\eta/\partial z$ and $\partial\zeta/\partial z$ are terms of the aforementioned J^{-1} matrix and given in App. I and all the other quantities are easily written in terms of (ξ,η,ζ) by differentiating the shape functions.
Similar considerations are valid for all the terms in J_A.

Integration procedure. Since the application "g" from a R^3 space to the isoparametric one is bijective and continuously differentiable, the integration of a function $f(x,y)$ can be carried into the isoparametric space,owing to the well known equality (ref.fig.3)

$$\int_A f(x,y)\,dx\,dy = \int_{A^*} f\,g(\xi,\eta)\,(\det J)\,d\xi\,d\eta \qquad (10)$$

where J is defined in (7).
Now,the (x,y) plane is normal to the crack front in P and contains nine Gauss Points in any element inside Γ (fig.4); since the F.E. results are relevant to a 3D mesh,the nine Gauss Points in question must be identified among the 27 Gauss Points of the element. The procedure is the following:

- definition of the isoparametric axes (ξ,η,ζ) on the basis of the connectivity of the element,by associating the directions according to the node sequence;
- numbering of the G.Points on the basis of the reference axes chosen;
- association of a real axis to an isoparametric axis.

The application of the Gaussian Quadrature method of integration can be applied directly solely to element F in fig.4; instead of the remaining elements in fig.4,we must consider modified tridimensional elements,where the external surface is limited by the integration path and,therefore,a new position of the Gauss Points occurs. In practice,a set of new elements is created.
The algorithms for the evaluation of GJ are implemented in a computer program in which the input data are the results of F.E. computations;in this research,the MARC code was used.

EXAMPLES OF APPLICATION

The utilization of GJ instead of S.I.F. as a measurement of Crack Driving Force allows us to obtain the following important advantages:

- it is possible to refer to a wider class of constitutive equations;the presence of non-elastic material around the crack front is allowed and stresses can be described by means of the Piola - Kirchhoff tensor as well;
- no hypothesis of plane stress or,alternatively, plane strain is needed,so relieving Fracture Mechanics of an unnecessary limitation.

Another important advantage will be seen in this paragraph,after the analysis of simple but interesting models:
- the computation of GJ by means of the F.E. method is easier than that of S.I.F.

The following models are considered:
A penny-shaped crack,
Elliptical embedded and surface cracks,
A Compact Tension specimen.

Penny-shaped crack model

The model is a cylinder,uniformly loaded in tension on the bases, where a central penny-shaped crack is present. Three different F.E. models have been considered,using twenty-node isoparametric elements and axialsymmetric elements;the mesh in fig.5 is relevant to a 1/8 of the body,with and without collapsed elements around the crack front.

Fig.6 shows some of the 36 integration paths considered together with the correspondent results;maximum and minimum values of GJ obtained are within $\pm$ 1.1 % of the average value.

The values of J_A cannot be disregarded with respect to J_L or,in other words,the plane strain condition is not fully satisfied; indeed,this situation cannot occur in an elastic boby.

In the Irwin's paper (7) the plane strain condition is assumed "a priori" as a consequence of the hypothesis that the crack contour does not move in its plane under the loading applied; clearly,this situation does not occur in any elastic body,where a crack shrinks monotonically under loading, Usually,the presence of plane strain state in 3D Fracture Mechanics is assumed in the presence of not well defined "large amount of material" around the crack ; this assumption seems to be rather arbitrary.

The results obtained show that the presence of collapsed elements in the crack front region does not play an important role as far as accuracy is concerned.

Elliptical embedded and surface cracks

The overall dimensions and loading conditions of the cracked body are the same as in the previous example; an elliptical crack,with a/c = 0.6,is present and the F.E. model of 1/8 of the body (fig.7) allows us to simulate the following conditions:

i) an internal elliptical crack,when symmetry conditions are prescribed on 3 planes;

ii) a surface elliptical crack,when symmetry is prescribed on two planes and free surface is imposed on the third plane.

Control points P_i are set in the middle of the sectors in fig.7; fig.8 shows the integration paths together with the values of GJ obtained and fig.9 shows the GJ values for elliptical internal and surface cracks.

It may be observed that:

- the values of GJ are invariant, even though J_A and J_L may vary when passing from one path to another (fig. 8 shows the results relevant to typical paths);
- the condition of pure plane strain is not satisfied and, therefore, no comparison is possible with results obtained in the plane strain hypothesis;
- no remarkable difference exists whether collapsed elements are used or not.

Compact Tension specimen

Compact Tension specimens are significant in Fracture Mechanics because they are a standard for assessing the Fracture Toughness of materials; the expression of S.I.F. in the literature concerns the plane strain condition and, therefore, the crack front is supposed to be straight.

Now, the following preliminary remarks are necessary:

i. the plane strain state cannot be present in the lateral faces, where $\sigma_z = 0$ (the z axis is set along the thickness),

ii. experiments show that the crack front grows faster in the middle of the thickness and, consequently, a certain gradient of the Crack Driving Force must be present when the crack front is straight

In the present analysis, a standard specimen is considered and three F.E. models are used primarily in order to improve the mesh refinement along the thickness; in fig. 10, 1/2 of the mesh is shown.

Fig. 10 shows a typical map of integration paths and certain results concerning model n. 1.

When the condition of symmetry is also prescribed in both the lateral planes, the effective plane strain condition is simulated.

Fig. 11 shows that, in this condition, the values of J_A become 10 orders of magnitude smaller than the previous ones; these results can be compared with those existing in the literature.

In particular, interesting research on a C.T. specimen was carried out by J.C.Newmann (8) using a Boundary Collocation method in plane strain conditions; the S.I.F. value obtained is : K = 1.035.

From the relationship:

$$GJ = \frac{1-\upsilon^2}{E} K^2 \tag{11}$$

we obtain K = 1.014 in the roughest mesh being considered.

In the experimental characterization of materials with respect to Fracture, a given material would seem to show different values of Fracture Thoughness K_C across the thickness of the C.T. specimen tested.

This situation is totally unsatisfactory; in the light of the present results, the stimulating conjecture may be made that the parameter chosen to provide a measurement of the toughness of a certain material is wrong and it is worthwhile trying to characterize materials in relation to their critical GJ values.

CONCLUSIONS

The Crack Driving Force at a point of a crack front can be written as the sum of a line integral,J_L,and a surface intagral,J_A; the quantity GJ = J_L-J_A has been called the "Generalized J Integral", because Rice's J Integral is a specification of GJ in the presence of plane stress or plane strain states (and,correspondently, J_A= 0)
The meaning of GJ is maintained even though non elastic material is present inside the integration path and stresses may depend on large deformations.
Both line and surface integrations can be carried out in the isoparametric space when twenty node isoparametric elements are used;in order to obtain this result,a suitable algorithm has been set up and implemented in a computer program.
A number of preliminary examples are discussed, viz.: a penny-shaped crack model,ellyptical embedded and surface cracks and a Compact Tension specimen.
The results obtained show that:
- a reliable evaluation of GJ is possible without a mesh refinement around the crack front and without collapsed elements;
- it is possible to give a quantitative evaluation of the presence of plane strain state on the basis of the value of J_A and the hypothesis of the presence of pure plane strain in Fracture Mechanics can be avoided;
- in the conditions where a comparison is possible,the present results are in agreement with those existing in the literature.

REFERENCES

(1) Rice,J.R.,j. Appl. Mechanics,No 35,1968,pp.379-386

(2) Kishimoto,K.,Aoki,S. and Sakata,M.,Engn.Fracture Mechanics,vol 13,1980,pp 841-850

(3) Frediani,A.,Lanciotti,A.,Vecchiatini,D.,L'Aerotecnica Missili e Spazio,Vol 63,No1,1984,pp19-28

(4) Bakker,A.,Elastic-Plastic Fracture Mechanics,June 1985,pp13-53

(5) Wang,G.,J.Aircraft,Vol 21,No 11,1984,pp 899-905

(6) Bennati,S.,to be presented at VIII Congress AIMETA Turin (Italy),Sept. 1986.

(7) Irwin,G.R.,J Applied Mechanics,Vol 84,No4,1962,pp 651-654

(8) Newman,J.C.,ASTM STP 560,1974,pp 105-121.

APPENDIX I

Calculation of the inverse of the Jacobian matrix

$$J^{-1} = \begin{bmatrix} \frac{\partial \xi}{\partial x} & \frac{\partial \eta}{\partial x} & \frac{\partial \zeta}{\partial x} \\ \frac{\partial \xi}{\partial y} & \frac{\partial \eta}{\partial y} & \frac{\partial \zeta}{\partial y} \\ \frac{\partial \xi}{\partial z} & \frac{\partial \eta}{\partial z} & \frac{\partial \zeta}{\partial z} \end{bmatrix}$$

We have,by definition:

$$J \cdot J^{-1} = I$$

or,in an expanded form

$$\frac{\partial x}{\partial \xi}\frac{\partial \xi}{\partial x} + \frac{\partial y}{\partial \xi}\frac{\partial \xi}{\partial y} + \frac{\partial z}{\partial \xi}\frac{\partial \xi}{\partial z} = 1$$

$$\frac{\partial x}{\partial \xi}\frac{\partial \eta}{\partial x} + \frac{\partial y}{\partial \xi}\frac{\partial \eta}{\partial y} + \frac{\partial z}{\partial \xi}\frac{\partial \eta}{\partial z} = 0$$

$$\frac{\partial x}{\partial \xi}\frac{\partial \zeta}{\partial x} + \frac{\partial y}{\partial \xi}\frac{\partial \zeta}{\partial y} + \frac{\partial z}{\partial \xi}\frac{\partial \zeta}{\partial z} = 0$$

$$\frac{\partial x}{\partial \eta}\frac{\partial \xi}{\partial x} + \frac{\partial y}{\partial \eta}\frac{\partial \xi}{\partial y} + \frac{\partial z}{\partial \eta}\frac{\partial \xi}{\partial z} = 0$$

$$\frac{\partial x}{\partial \eta}\frac{\partial \eta}{\partial x} + \frac{\partial y}{\partial \eta}\frac{\partial \eta}{\partial y} + \frac{\partial z}{\partial \eta}\frac{\partial \eta}{\partial z} = 1$$

$$\frac{\partial x}{\partial \eta}\frac{\partial \zeta}{\partial x} + \frac{\partial y}{\partial \eta}\frac{\partial \zeta}{\partial y} + \frac{\partial z}{\partial \eta}\frac{\partial \zeta}{\partial z} = 0$$

$$\frac{\partial x}{\partial \zeta}\frac{\partial \xi}{\partial x} + \frac{\partial y}{\partial \zeta}\frac{\partial \xi}{\partial y} + \frac{\partial z}{\partial \zeta}\frac{\partial \xi}{\partial z} = 0$$

$$\frac{\partial x}{\partial \zeta}\frac{\partial \eta}{\partial x} + \frac{\partial y}{\partial \zeta}\frac{\partial \eta}{\partial y} + \frac{\partial z}{\partial \zeta}\frac{\partial \eta}{\partial z} = 0$$

$$\frac{\partial x}{\partial \zeta}\frac{\partial \zeta}{\partial x} + \frac{\partial y}{\partial \zeta}\frac{\partial \zeta}{\partial y} + \frac{\partial z}{\partial \zeta}\frac{\partial \zeta}{\partial z} = 1$$

This set of equations can be divided into three subsets of equations; they can be solved singly and the result is

$$\frac{\partial \xi}{\partial x} = \frac{\frac{\partial y}{\partial \eta}\frac{\partial z}{\partial \zeta} - \frac{\partial y}{\partial \zeta}\frac{\partial z}{\partial \eta}}{|J|} \qquad \frac{\partial \zeta}{\partial y} = \frac{\frac{\partial x}{\partial \eta}\frac{\partial z}{\partial \xi} - \frac{\partial x}{\partial \xi}\frac{\partial z}{\partial \eta}}{|J|}$$

$$\frac{\partial \eta}{\partial x} = \frac{\frac{\partial y}{\partial \zeta}\frac{\partial z}{\partial \xi} - \frac{\partial y}{\partial \xi}\frac{\partial z}{\partial \zeta}}{|J|} \qquad \frac{\partial \xi}{\partial z} = \frac{\frac{\partial x}{\partial \eta}\frac{\partial y}{\partial \zeta} - \frac{\partial x}{\partial \zeta}\frac{\partial y}{\partial \eta}}{|J|} = \frac{a}{|J|}$$

$$\frac{\partial \zeta}{\partial x} = \frac{\frac{\partial y}{\partial \xi}\frac{\partial z}{\partial \eta} - \frac{\partial y}{\partial \eta}\frac{\partial z}{\partial \xi}}{|J|} \qquad \frac{\partial \eta}{\partial z} = \frac{\frac{\partial x}{\partial \zeta}\frac{\partial y}{\partial \xi} - \frac{\partial x}{\partial \xi}\frac{\partial y}{\partial \zeta}}{|J|} = \frac{b}{|J|}$$

$$\frac{\partial \xi}{\partial y} = \frac{\frac{\partial x}{\partial \zeta}\frac{\partial z}{\partial \eta} - \frac{\partial x}{\partial \eta}\frac{\partial z}{\partial \zeta}}{|J|} \qquad \frac{\partial \zeta}{\partial z} = \frac{\frac{\partial x}{\partial \xi}\frac{\partial y}{\partial \eta} - \frac{\partial x}{\partial \eta}\frac{\partial y}{\partial \xi}}{|J|} = \frac{c}{|J|};$$

$$\frac{\partial \eta}{\partial y} = \frac{\frac{\partial x}{\partial \xi}\frac{\partial z}{\partial \zeta} - \frac{\partial x}{\partial \zeta}\frac{\partial z}{\partial \xi}}{|J|}$$

where:

$$a = \frac{\partial x}{\partial \eta}\frac{\partial y}{\partial \zeta} - \frac{\partial x}{\partial \zeta}\frac{\partial y}{\partial \eta}\,;\; b = \frac{\partial x}{\partial \zeta}\frac{\partial y}{\partial \xi} - \frac{\partial x}{\partial \xi}\frac{\partial y}{\partial \zeta}\,;\; c = \frac{\partial x}{\partial \xi}\frac{\partial y}{\partial \eta} - \frac{\partial x}{\partial \eta}\frac{\partial y}{\partial \xi};$$

$$|J| = \frac{\partial z}{\partial \xi}\left(\frac{\partial x}{\partial \eta}\frac{\partial y}{\partial \zeta} - \frac{\partial x}{\partial \zeta}\frac{\partial y}{\partial \eta}\right) + \frac{\partial z}{\partial \eta}\left(\frac{\partial x}{\partial \zeta}\frac{\partial y}{\partial \xi} - \frac{\partial x}{\partial \xi}\frac{\partial y}{\partial \zeta}\right) +$$

$$+ \frac{\partial z}{\partial \zeta}\left(\frac{\partial x}{\partial \xi}\frac{\partial y}{\partial \eta} - \frac{\partial x}{\partial \eta}\frac{\partial y}{\partial \xi}\right) =$$

$$= \frac{\partial z}{\partial \xi}\,a + \frac{\partial z}{\partial \eta}\,b + \frac{\partial z}{\partial \zeta}\,c$$

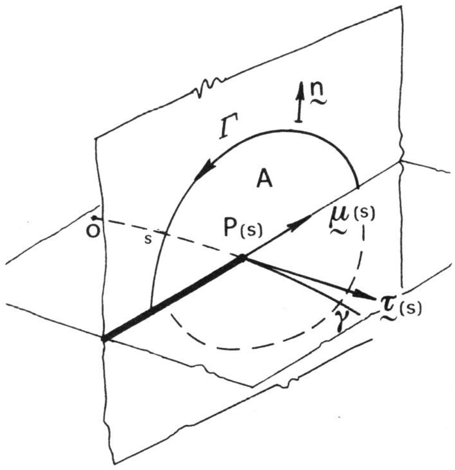

Fig.1 Sketch of the notations used

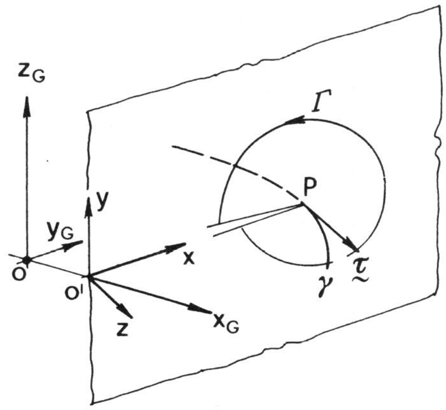

Fig.2 Global and local reference systems.

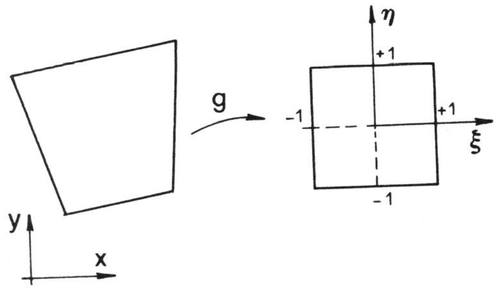

Fig.3 Application from R^3 to the isoparametric space

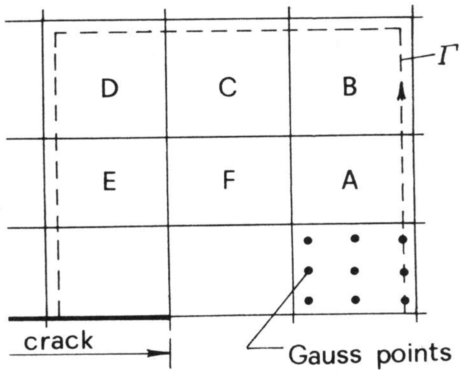

Fig.4 Typical integration path.

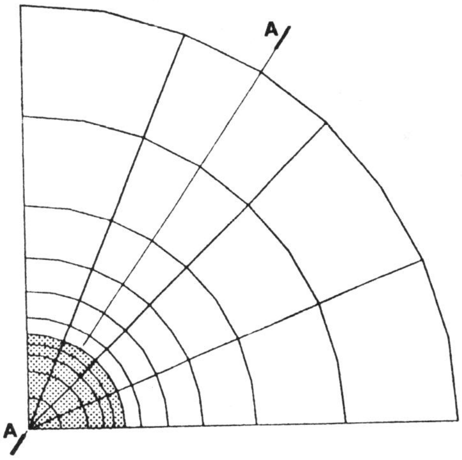

Fig.5 Central section of the penny-shaped crack model

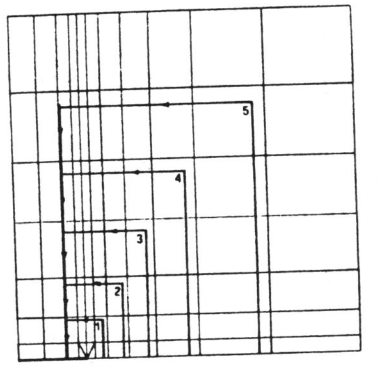

Path	J_L	J_A	$GJ = J_L - J_A$
1	0.55681×10^{-2}	0.12293×10^{-2}	0.43387×10^{-2}
2	0.61028×10^{-2}	0.17595×10^{-2}	0.43343×10^{-2}
3	0.63316×10^{-2}	0.19860×10^{-2}	0.43456×10^{-2}
4	0.64135×10^{-2}	0.20641×10^{-2}	0.43493×10^{-2}

Fig.6 Values of GJ of the penny-shaped crack

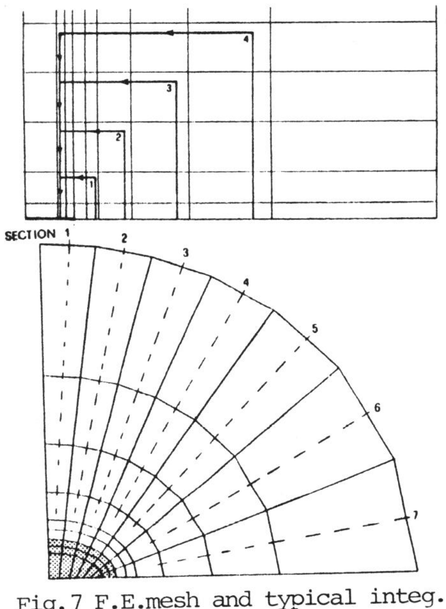

Fig.7 F.E.mesh and typical integ. paths of elliptical crack.

SECTION	Path	J_L	J_A	$GJ = J_L - J_A$
1	1	0.544×10^{-3}	0.358×10^{-4}	0.508×10^{-3}
	2	0.568×10^{-3}	0.568×10^{-4}	0.511×10^{-3}
	3	0.577×10^{-3}	0.654×10^{-4}	0.512×10^{-3}
	4	0.581×10^{-3}	0.688×10^{-4}	0.512×10^{-3}
2	1	0.532×10^{-3}	0.389×10^{-4}	0.493×10^{-3}
	2	0.555×10^{-3}	0.595×10^{-4}	0.496×10^{-3}
	3	0.564×10^{-3}	0.676×10^{-4}	0.496×10^{-3}
	4	0.567×10^{-3}	0.708×10^{-4}	0.497×10^{-3}
3	1	0.508×10^{-3}	0.452×10^{-4}	0.464×10^{-3}
	2	0.531×10^{-3}	0.647×10^{-4}	0.467×10^{-3}
	3	0.539×10^{-3}	0.719×10^{-4}	0.467×10^{-3}
	4	0.543×10^{-3}	0.749×10^{-4}	0.468×10^{-3}
4	1	0.481×10^{-3}	0.554×10^{-4}	0.425×10^{-3}
	2	0.502×10^{-3}	0.740×10^{-4}	0.428×10^{-3}
	3	0.510×10^{-3}	0.805×10^{-4}	0.429×10^{-3}
	4	0.512×10^{-3}	0.832×10^{-4}	0.429×10^{-3}
5	1	0.453×10^{-3}	0.689×10^{-4}	0.384×10^{-3}
	2	0.475×10^{-3}	0.873×10^{-4}	0.387×10^{-3}
	3	0.482×10^{-3}	0.936×10^{-4}	0.388×10^{-3}
	4	0.484×10^{-3}	0.962×10^{-4}	0.388×10^{-3}
6	1	0.434×10^{-3}	0.870×10^{-4}	0.347×10^{-3}
	2	0.458×10^{-3}	0.107×10^{-3}	0.351×10^{-3}
	3	0.465×10^{-3}	0.114×10^{-3}	0.351×10^{-3}
	4	0.468×10^{-3}	0.117×10^{-3}	0.351×10^{-3}
7	1	0.427×10^{-3}	0.101×10^{-3}	0.325×10^{-3}
	2	0.453×10^{-3}	0.123×10^{-3}	0.329×10^{-2}
	3	0.461×10^{-3}	0.131×10^{-3}	0.330×10^{-3}
	4	0.464×10^{-3}	0.134×10^{-3}	0.330×10^{-3}

Fig.8 Typical GJ results

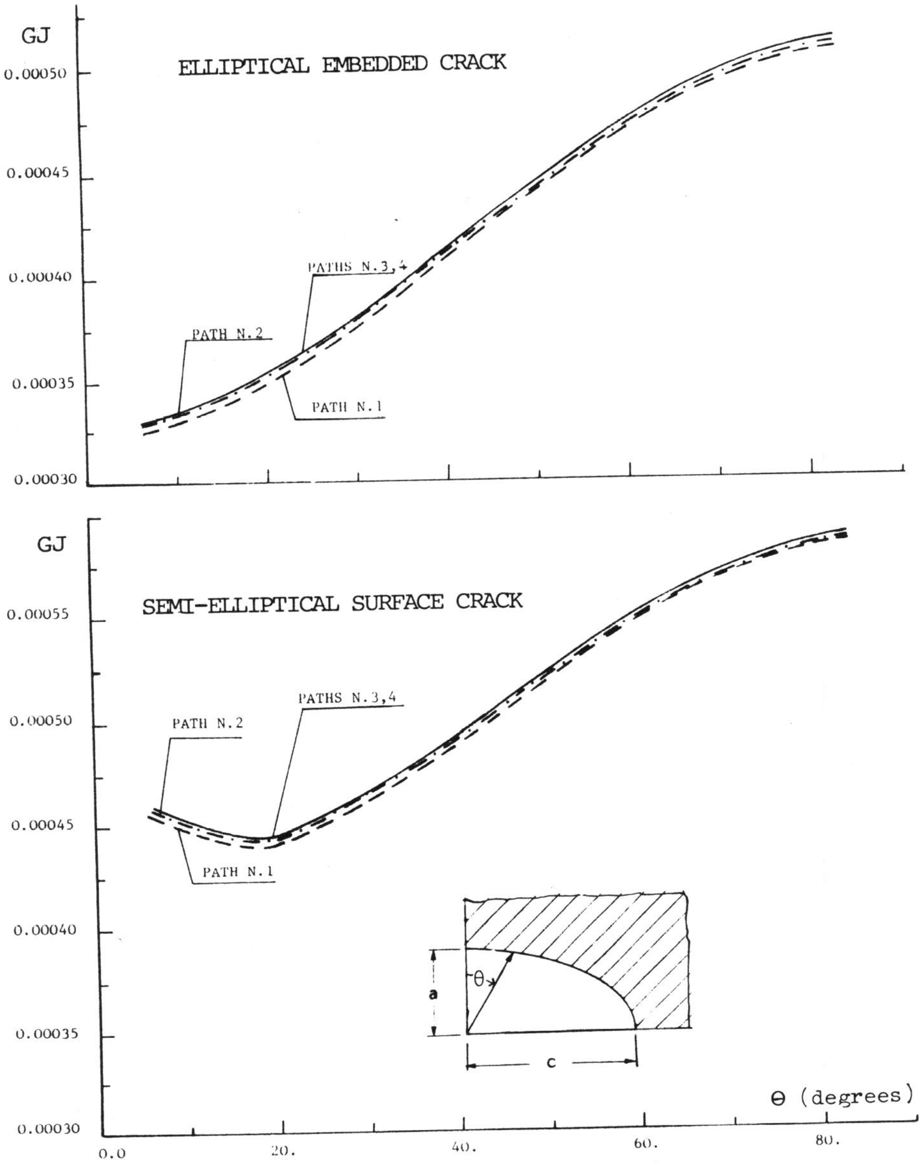

Fig.9 GJ values relevant to elliptical embedded crack and semi-elliptical surface crack

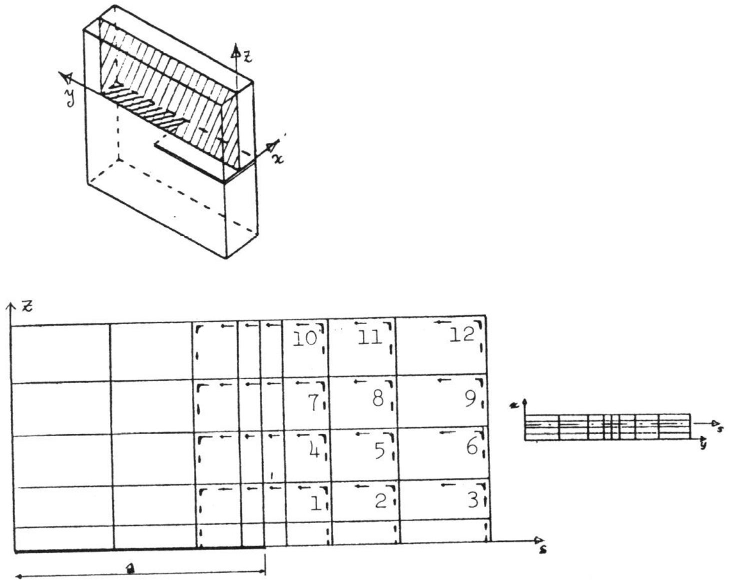

Fig.10 Typical integration paths
for the C.T.specimen.

PATH No.	J_A	J_L	GJ	K plane strain
1	-0.312836D-12	0.128740D-03	0.128740D-03	0.101276D+01
2	-0.312759D-12	0.129254D-03	0.129254D-03	0.101478D+01
3	-0.312744D-12	0.129314D-03	0.129314D-03	0.101501D+01
4	0.543384D-14	0.128578D-03	0.128578D-03	0.101212D+01
5	0.560785D-14	0.128907D-03	0.128907D-03	0.101341D+01
6	0.559843D-14	0.129947D-03	0.129947D-03	0.101749D+01
7	0.875754D-13	0.128873D-03	0.128873D-03	0.101328D+01
8	0.878092D-13	0.129109D-03	0.129109D-03	0.101421D+01
9	0.877772D-13	0.131160D-03	0.131160D-03	0.102223D+01
10	-0.234326D-12	0.127079D-03	0.127079D-03	0.100620D+01
11	-0.234012D-12	0.127616D-03	0.127616D-03	0.100833D+01
12	-0.234045D-12	0.130106D-03	0.130106D-03	0.101812D+01

Fig.11 Typical output of the computer program